Earthquake Geotechnical Engineering for Protection and Development of Environment and Constructions – Silvestri & Moraci (Eds)
© 2019 Associazione Geotecnica Italiana, Rome, Italy, ISBN 978-0-367-14328-2

Ultimate design capacity of bridge abutments

D.N. Gorini & L. Callisto
Sapienza University of Rome, Rome, Italy

A.J. Whittle
Massachusetts Institute of Technology, Cambridge, MA, USA

ABSTRACT: Under the large forces transmitted by a bridge structure during an earthquake, a bridge abutment may undergo significant displacements deriving from the mobilisation of both the soil and the structural strength. In some cases a controlled yielding of the abutment may produce favourable effects, dissipating seismic energy and limiting the seismic actions into the superstructure. In fact, the bridge design could explicitly account for dissipative features of the soil-abutment system, allowing a certain amount of irreversible displacements compatible with a prescribed performance level. The present paper focuses on the plastic response of the soil-abutment system, examining its potential plastic mechanisms. With the aid of numerically-evaluated limit analysis solutions, different plastic mechanisms are identified, including those associated with combined yielding of the soil and the abutment structure. On the basis of the above results, the paper presents a model describing the capacity surface of bridge abutments subjected to multi-axial loading conditions, that can be identified through the calibration of a limited number of parameters. It is shown that the inertial effects associated to the seismic loading can be incorporated into the model through a contraction and a rotation of the ultimate limit surface. The proposed model can be either included in a plasticity-based macro-element to model the bridge abutments, or it can be used for a direct evaluation of abutment in a force-based approach.

1 THE NONLINEAR BEHAVIOUR OF BRIDGE ABUTMENTS

A bridge abutment can exhibit a marked nonlinear response under severe ground shaking. The nonlinear features of the behaviour of the soil-abutment system might be regarded as an intrinsic dissipative source for a bridge, with a consequent limitation of the seismic actions transferred to the superstructure through the temporary attainment of the ultimate capacity of the system.

In recent years, the nonlinear behaviour of the soil-abutment system was analysed in some experimental load tests (Romstad et al. 1995, Gadre and Dobry 1998, Stewart et al. 2007), that were aimed to study the progressive mobilization of the passive resistance in the backfill induced by a purely longitudinal force applied to the top of the abutment. Afterwards, Shamsabadi et al. (2007) proposed a model to predict the longitudinal response of seat-type bridge abutments towards passive earth pressure conditions, in which the pronounced nonlinear behaviour of the system, from small strains up to failure, was reproduced through a hyperbolic law. A relevant source of energy dissipation for an abutment can be also represented by the full-strength mobilisation in the soil and in the foundation piles during the earthquake (Callisto and Rampello 2013).

The capacity of an abutment is dependent on the direction of the loads deriving from the bridge deck and from the backfill. This is illustrated in the following by the results of a study on the ultimate conditions of bridge abutments under multi-axial loading.

2 LIMIT ANALYSIS AND NUMERICAL MODELLING

The capacity of bridge abutments under general loading paths was analysed with finite element simulations of limit analysis (Sloan 1988, 1989) using the software Optum G3 (OptumCE 2016). Lower and upper bound solutions were evaluated on local models of abutments such as that shown in Figure 1.

Each element of the domain was modelled as a solid element characterized by a perfectly plastic behaviour described by the Mohr-Coulomb failure criterion with an associated flow rule. The domain includes the abutment, the embankment and the foundation soil. The contact between the structure and the soil is modelled by means of thin layers meshed by solid elements with appropriate strength properties (see Section 3). In the numerical simulations, the external perturbation consists of a set of distributed forces applied to the top of the central wall in the three translational degrees of freedom of the deck-abutment contact, representative of the load coming from the deck, whose positive signs are shown in Figure 1. The moment transmission on the abutment top is not considered because it was found in preliminary studies that for non-integral bridges it has a limited effect on the ultimate conditions. The numerical simulations provide the intensity of the external forces that causes the failure of the system. Each analysis is composed of several iterations with mesh adaptivity in order to concentrate the discretization of the domain where plastic strains occur, in such a way that the upper and lower bound solutions become nearly coincident. The results shown in the following are relative to the upper bound solutions to also analyse the kinematics associated with the plastic modes. The failure loads are expressed in terms of forces per unit length of the central wall.

3 ULTIMATE SURFACE FOR ABUTMENTS WITH SHALLOW FOUNDATIONS

Consider an abutment subjected to a combined longitudinal Q_1, transverse Q_2 and vertical Q_3 load applied to the deck-abutment contact. The geometry of the abutment is inspired by the case study of the Pantano viaduct in Italy (Gorini and Callisto 2017), with a 13.5 m-height wall and a length of the foundation slab of 17.5 m and 20.0 m, in the longitudinal and transverse directions, respectively. In this reference configuration, the abutment is regarded as a rigid body with a unit weight of 25 kN/m^3. The foundation soil and the embankment, assumed dry, have an angle of shearing resistance of 30° and a unit weight of 20 kN/m^3. The interface elements are characterized by the same friction angle as the soil, representing a reasonable assumption for a soil-concrete contact. Two different cases are examined, making use of either shallow or deep foundations.

Figure 2 summarizes the results for a shallow foundation system. The computed results are represented in the forces spaces, (Q_1,Q_3) and (Q_2,Q_3), each point represents a combination of

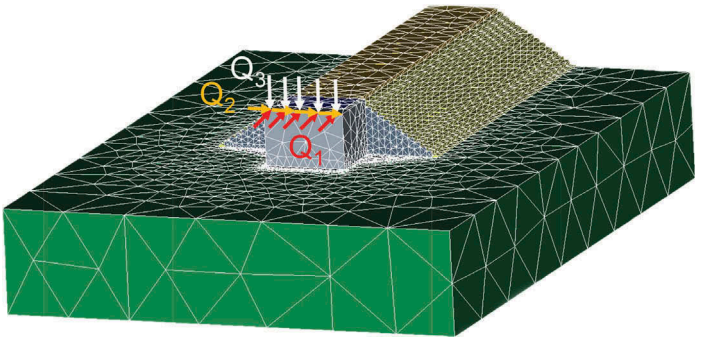

Figure 1. Three dimensional model implemented in Optum G3 and positive signs of the forces applied to the abutment.

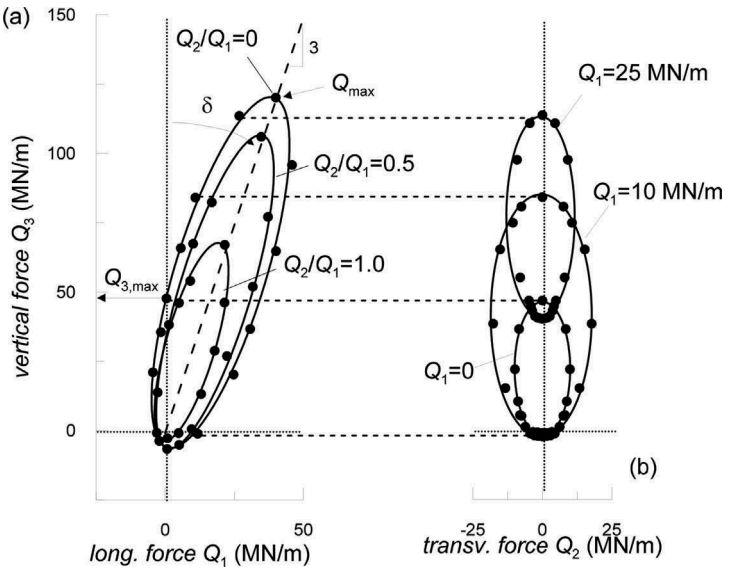

Figure 2. (a) Traces of the ultimate surface in the plane (Q_1,Q_3) obtained through three-dimensional simulations for different values of the skew load ratio Q_2/Q_1; (b) traces of the surface in the plane (Q_2,Q_3).

the three applied loads activating a global plastic mechanism. In Figure 2(a) it is evident that, for each load ratio Q_1/Q_3, the failure points can be well described by an ellipse, characterized by a specific orientation δ with respect to the vertical axis Q_3 that identifies the ratio Q_1/Q_3 corresponding to the maximum capacity Q_{max}. The ellipse is almost entirely located in the first quadrant of the positive forces, reflecting the highly asymmetric response of the abutment: the simultaneous application of the two components of the load leads to a noticeable increase of the capacity when the forces are directed downwards and towards the backfill while it causes a drastic reduction of the resistance when they push away the abutment from the soil. When a transverse force Q_2 is also applied to the central wall, the size of the limit locus reduces progressively with the skew ratio, Q_2/Q_1, but the ellipse maintains the same orientation. Moreover, looking at the effect of the transverse force in the transverse-vertical plane, illustrated in Figure 2(b), it is evident that every ultimate locus can be again represented by an ellipse with different size.

Accordingly, the ultimate surface of an abutment can be described by an ellipsoid, almost entirely located in the first quadrant and inclined with respect to the coordinate axes, whose analytical expression reads:

$$\frac{[(Q_3 - c_3)\cos(\delta) + (Q_1 - c_1)\sin(\delta)]^2}{a_M^2} + \frac{Q_2^2}{a_i^2} + \frac{[-(Q_3 - c_3)\sin(\delta) + (Q_1 - c_1)\ \cos(\delta)]^2}{a_m^2} - 1 = 0$$

The ellipsoid is centred at C = (c_1,0, c_3) and is rotated by an angle $\delta = \arctan(Q_1/Q_3)$ in the plane (Q_1,Q_3). It is symmetric with respect to the Q_2-axis for the symmetry of the problem. The major semi-axis is denoted as a_M, the minor one a_m while a_i indicates the intermediate value.

The ellipsoid can be completely identified through the maximum resultant force Q_{max}, depending on the soil strength and the abutment geometry, and trough the angle δ, that is mainly controlled by the friction angle at the soil-structure contact. The maximum capacity can be related to the vertical limit load $Q_{3,max}$ representing the bearing capacity of the foundation for a vertical load applied at the deck-abutment contact: a parametric study on failure conditions showed that the ratio $Q_{max}/Q_{3,max}$ ranges between 3.0 and 3.5.

4 INERTIAL EFFECTS ON THE ULTIMATE CAPACITY

Under seismic conditions, the inertial effects that develop in the soil and the abutment can alter the activation of the plastic mechanisms of the system. A simplified method to study this phenomenon consists in representing the effects induced by the seismic excitation through pseudo-static forces. The latter are reproduced in a plane-strain limit analysis (software Optum G2) as a uniform field of acceleration, considered purely horizontal, applied to the entire domain through the seismic coefficient k_h (in the simulations k_h is taken as positive when the inertial forces are directed towards the backfill).

Figure 3 shows the traces of the failure surface in the Q_1-Q_3 plane for different values of k_h. It is evident that the inertial forces cause a contraction and a rotation of the limit surface, without altering its shape. The dimension of the admissible domain always reduces as the

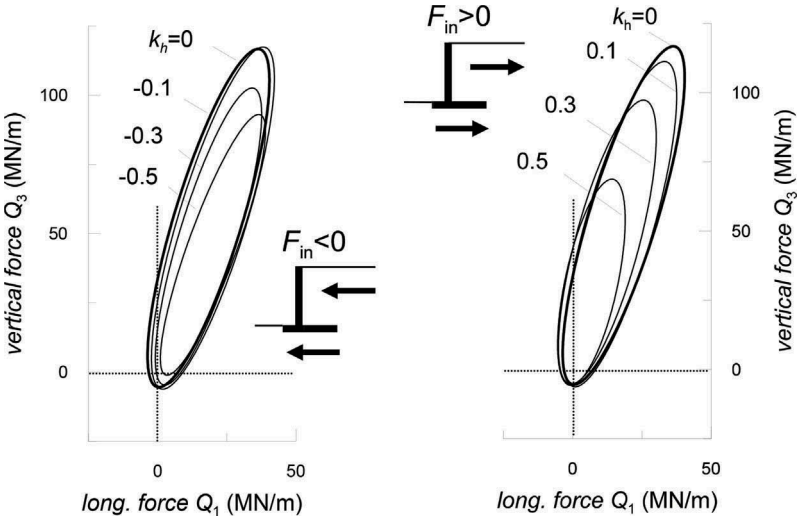

Figure 3. Inertial effects: comparison between the ultimate surface retrieved under static conditions (k_h = 0) and those related to different values of the seismic coefficient (k_h > 0 if directed towards the backfill).

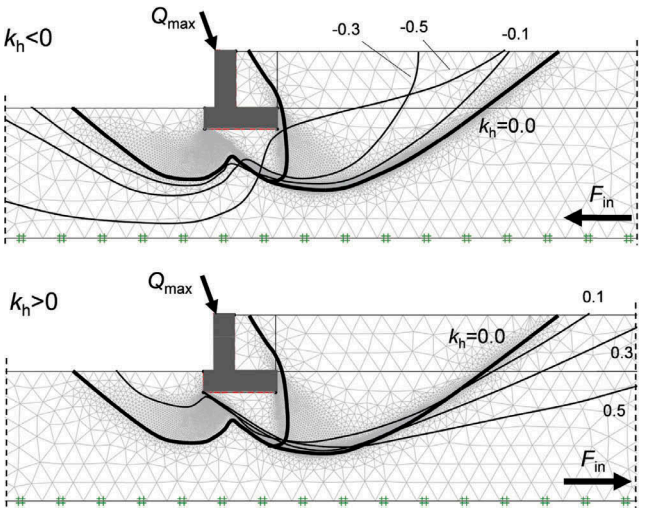

Figure 4. Effect of the seismic coefficient k_h on the global plastic mechanisms corresponding to the maximum capacity of the soil-abutment system.

seismic coefficient rises but this is more evident when the inertial forces are directed towards the backfill ($k_h > 0$), because they favour the activation of the plastic mechanism associated with the maximum capacity. The corresponding sliding surfaces, depicted in Figure 4, move progressively upstream when the pseudo-static forces are directed towards the backfill, while the opposite occurs when the inertial forces are directed away from the backfill.

5 COMBINED SOIL-STRUCTURE FAILURE

The preceding results involve plastic failure mechanisms in the embankment and foundation soils, while the abutment structure undergoes rigid body deformations. Combined soil-structure failure will occur when the abutment is supported on pile foundations.

5.1 *Abutments with deep foundations*

The plastic behaviour of piles was described by means of an equivalent Mohr-Coulomb criterion (Pujol et al. 2016). The piles are made of reinforced concrete and were modelled as solid elements in Optum G3, in order to reproduce the effective plastic flow of the soil between the piles and to detect the local mobilisation of the structural strength along the shaft. The spacing of the piles group, normalised with respect to the pile diameter D_p, in the longitudinal and transverse directions are $i_{long}/D_p = 3.5$ and $i_{tr}/D_p = 3.3$, respectively. The equivalent cohesion and angle of shearing resistance are equal to 5000 kPa and 55°, respectively. The soil-pile interface was modelled through thin layers interposed between the soil and the structural members, having the same strength parameters as those of the soil assuming cast-in-place concrete piles.

Looking at the ultimate surfaces shown in the Q_1-Q_3 plane of Figure 5, it can be seen that the ultimate locus of an abutment with deep foundation can still be represented by the capacity model illustrated in the previous section. In particular, Figure 5(a) compares the capacity of the reference abutment with a shallow foundation with that of the piled foundation for two different pile lengths L_p, equal to 18.5 and 5.0 times the pile diameter. It is evident that the piles do not change

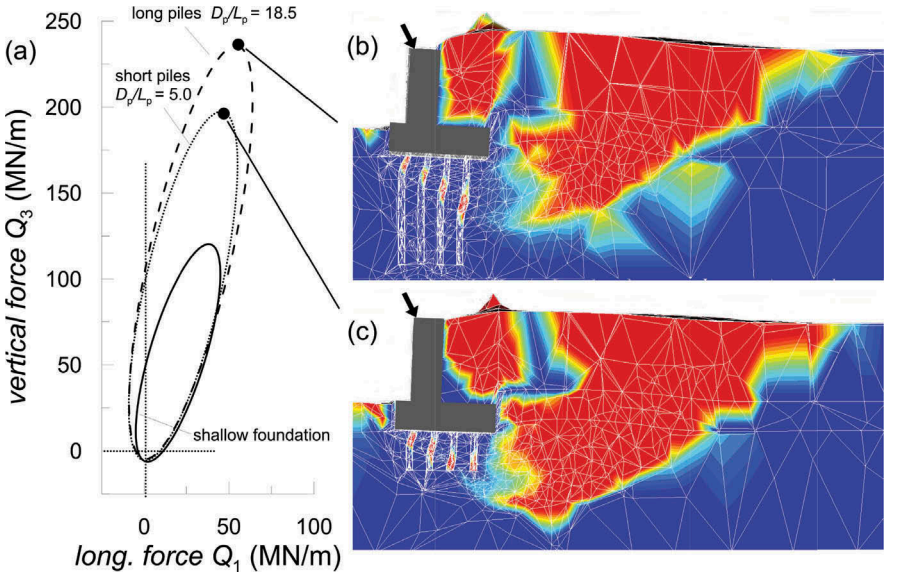

Figure 5. Three-dimensional failure of an abutment with deep foundation: (a) surface of ultimate loads for a rigid abutment founded on a group of short piles with L_{pile}/D_{pile}=5.0, L_{pile}/H=1.4 (dotted line) and a group of long piles with L_{pile}/D_{pile} =18.5 and L_{pile}/H =3.4 (dashed line); plastic mechanisms occurring at the maximum capacity for long (b) and short (c) piles.

the shape of the ultimate surface but they confer a higher capacity to the abutment. The capacity increases with the pile length, especially in the region where the abutment exhibits the maximum capacity. Looking at the plastic mechanisms activated by the maximum capacity (Figure 5(b,c)) for these fixed head piles, a first hinge forms at the foundation connection only for the piles on the downstream side, while another hinge is found for all the piles at depths that vary from the toe to the heel of the foundation. For the short piles instead, an intermediate mechanism occurs: the sliding surface passes through the first two rows, with formation of two hinges along the stem, whereas the strength of the piles on the upstream side is attained in proximity of the pile tip.

The presence of an additional transverse force Q_2 leads to a contraction of the ultimate locus in the plane (Q_1,Q_3), as illustrated in Figure 6. Although the reduction of capacity is more pronounced in the case of long piles, the reduction ratio is nearly identical between the two cases. This behaviour is conceptually identical to that observed for an abutment with shallow foundation, validating the formulation proposed to describe the multi-axial capacity of bridge abutments.

5.2 *Abutments with piles isolated from abutment foundation*

In the case of abutments with deep foundations, the seismic actions transmitted to the superstructure might be limited by inserting a frictional device into a piled foundation, at the contact of the piles with the connecting cap. This allows a controlled sliding when the seismic forces reach a given critical value, that should be chosen to provide a desired seismic performance of the structure. This type of dissipative foundation was adopted for the towers of two recent long-span bridges, namely the Rion Antirion cable stayed bridge in Greece (Pecker 2003) and the Izmit Bay suspension bridge in Turkey (Zhang et al. 2013, Gorini and Callisto 2015, Gorini and Callisto 2016). This solution might be conceptually employed also in the case of a piled bridge abutment as a base isolation system for the foundation.

Consider a frictional interface inserted between the piles and the base of the abutment, characterised by a friction angle $\varphi_{int,diss}$. Figure 7 shows the envelopes of the ultimate surfaces of the abutment, evaluated through limit analysis, for the two different pile length of 5 diameters (short piles) and 18.5 diameters (long piles) and considering different values of the friction angle of the dissipative interface $\varphi_{int,diss}$=30°, 20°, 10°. The most evident result is that, for a given value of $\varphi_{int,diss}$, the corresponding limit surface does not depend significantly on the length of the piles. This can be explained looking at the plastic mechanism depicted in Figure 8, corresponding to the attainment of the maximum capacity Q_{max} and for a friction angle $\varphi_{int,diss}$=10°: the strength is mobilised along the frictional interface and the piles are not involved in the plastic mechanism. When the friction angle of the soil-pile interface is equal to that of the soil, $\varphi_{int,diss}=\varphi_{soil}$=30°, the ultimate surface in the case of long piles is essentially identical to that obtained for the short piles, which in turn exhibits the same capacity as the abutment with fully connected piles. In this case, for the short piles, the angle of friction at the pile-base contact is too large to modify substantially the global plastic mechanisms. If the use of a dissipative interface is aimed to reduce the seismic forces transmitted to the structure, it appears more effective in the case of long piles. For the case examined above, a substantial reduction of the friction angle at the foundation-pile interface can lead to a significant reduction of Q_{max} up to about 35 %, compared to the case of piles fully connected to the foundation.

6 CONCLUSIONS

The proposed model of ultimate capacity for a bridge abutment subjected to multi-axial loading defines the maximum interaction forces that can be exchanged at the deck-abutment contact, that in turn are the maximum loads that can be taken by the superstructure of the bridge during a seismic event. These forces are associated with the mobilisation of global plastic mechanisms of the abutment and therefore depend on the strength of the soil-abutment system. In the case of deep foundations, in fact, it was shown that the ultimate resistance of an abutment can be controlled by an adequate choice of the geometry and strength of the piles.

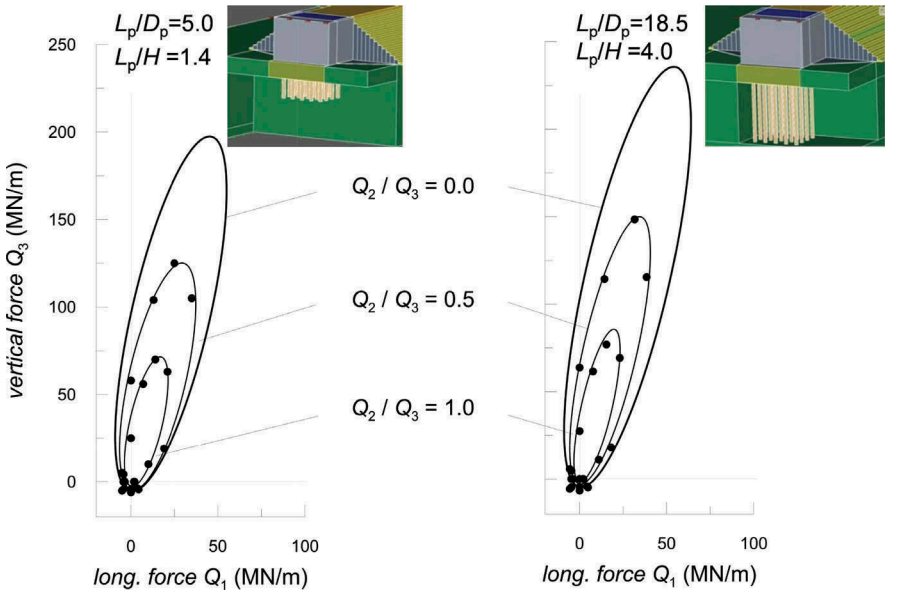

Figure 6. Comparison between the abutment founded on short piles and on long piles: traces of the surface of ultimate loads in the Q_1-Q_3 plane, for different levels of the transverse force applied to the abutment top.

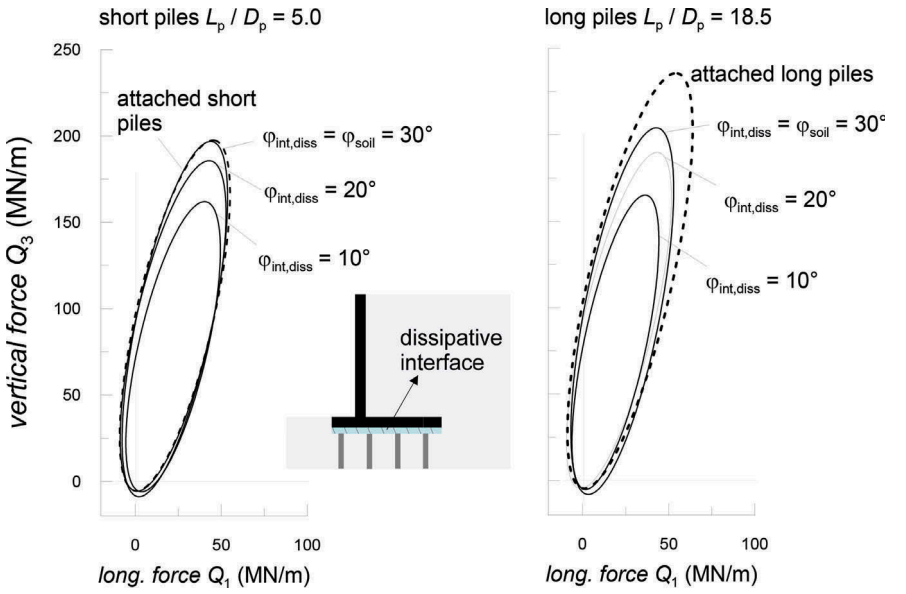

Figure 7. Influence of the friction angle $\varphi_{int,diss}$ of the dissipative pile-foundation interface on the capacity of the soil-abutment system for a slenderness ratio of the piles L_p/D_p equal to 5.0 and 18.5.

The ultimate capacity of an abutment is also altered by the inertial effects that develop under seismic conditions. The resulting contraction of the ultimate surface of the soil-abutment system, that is proportional to the intensity of the seismic motion, is also associated with a rotation of the limit locus, whose direction changes according to how the seismic motion combines with the inertial forces transferred by the deck, leading to an ultimate capacity that depends not only on the load direction but that is also a function of time.

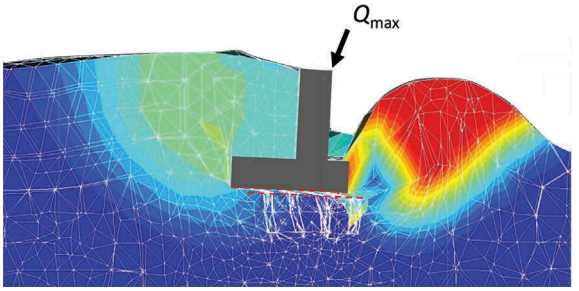

Figure 8. Deformed shape of the central section of the soil-abutment model obtained for a friction angle along the soil-pile interface of 10° and in correspondence of the maximum capacity (Q_3/Q_1 =3).

The identification of an ultimate plastic domain for an abutment is useful to extend the current principles of capacity design of bridges, in which the dissipative behaviour of the soil-abutment system could play a key role in controlling the seismic performance of the bridge. In this view, the capacity model can be also regarded as an efficient tool for structural analysis, as a part of a plasticity-based macro-element of the soil-abutment system, to evaluate the effectiveness of these local dissipative mechanisms on the seismic performance of the whole bridge structure.

REFERENCES

Callisto, L., & Rampello, S. 2013. Capacity design of retaining structures and bridge abutments with deep foundations. *J. Geotech. Geoenviron. Eng*. 139(7): 1085–1095.

Gadre, A.D., & Dobry, R. 1998. Centrifuge modeling of cyclic lateral response of pile cap systems and seat-type abutments in dry sand." *Rep. MCEER-98-0010, Rensselaer Institute, Civil Engineering Dept.*, Troy, N.Y.

Gorini D.N., & Callisto, L. 2015. Dynamic soil-structure interaction for a long-span suspension bridge with dissipative foundations. *In*: *Proc. of the 4th International Workshop on Dynamic Interaction of Soil and Structure (DISS 15)*, ISBN: 978-88-940114-2-5, 11: 289–297.

Gorini D.N., & Callisto, L. 2016. Predicting the dynamic response of friction dissipative foundations using a modifed Newmark model. *Procedia Engineering* 158: 170–175.

Gorini D.N., & Callisto, L. 2017. Study of the dynamic soil-abutment-superstructure interaction for a bridge abutment. *Proc. 1st European Conference on OpenSees (OpenSees Days Europe 2017)* 57-60, ISBN 978-972-752-221-7, Porto, Portugal.

OptumCE 2016. OptumG2 v. 2016. Manual. https://optumce.com/products/brochure-and-datasheet/.

Pecker, A. 2003. Aseismic foundation design process, lessons learned from two major projects: 18 the Vasco de Gama and the Rion Antirion bridges. *In: ACI Int. Conf. Seismic Bridge 19 Design & Retro t*, La Jolla, California.

Pujol, S., Hanai, N., Ichinose, T., & Sozen M.A. 2016. Using Mohr-Coulomb criterion to estimate shear strength of reinforced concrete columns. *ACI Structural Journal* 113: 459–468.

Romstad, K., Kutter, B., Maroney, B., Vanderbilt, E., Griggs, M., & Chai, Y.H. 1995. Experimental measurements of bridge abutment behavior. *Rep. No. UCD-STR-95-1, Dept. of Civil and Environmental Eng*., *Univ. of California*, Davis, California.

Shamsabadi, A., Rollins, K.M., & Kapuskar, M. 2007. Nonlinear soil-abutment-bridge structure interaction for seismic performance based design. *J. Geotech. Geoenviron. Eng*. 1336: 707–720.

Sloan, S.W. 1988. Lower bound limit analysis using finite elements and linear programming. *Int. J. Numer. Anal. Methods Geomech*. 12: 61–67.

Sloan, S.W. 1989. Lower bound limit analysis using finite elements and linear programming. *Int. J. Numer. Anal. Methods Geomech*. 13: 263–282.

Stewart, J.P., Taciroglu, E., Wallace, J.W., Ahlberg, E.R., Lemnitzer, A., Rha, C., & Tehrani, P.K. 2007. Full scale cyclic testing of foundation support systems for highway bridges. Part II: Abutment backwalls. *Rep. No. UCLA-SGEL- 2007/02, Structural and Geotechnical Engineering Laboratory*, *Univ. of Calif*., Los Angeles, California.

Zhang, Y., Yao, S., & Christie, S.R. 2013. Non-linear and equivalent linear site response analysis for 15 the Izmit Bay bridge. *In: Proc. 3rd International FLAC/DEM Symposium*, Hangzhou, paper 05/2.